J|A|C|S
COMMUNICATIONS

Published on Web 08/16/2002

Reintroducing Anisotropic Interactions in Magic-Angle-Spinning NMR of Half-Integer Quadrupolar Nuclei: 3D MQMAS†

Sungsool Wi, Henrike Heise, and Alexander Pines*

Materials Sciences Division, Lawrence Berkeley National Laboratory and Department of Chemistry, University of California at Berkeley, Berkeley, California 94720

Received May 24, 2002

The majority (72%) of the magnetically active nuclides in the periodic table possess half-integer spins higher than 1.[1] Hence, solid-state NMR methods that provide not only site-specific resolution but also dipolar coupling and chemical shift information of half-integer quadrupolar nuclei are enormously useful to fully characterize the structural properties. High-resolution spectra of half-integer quadrupolar nuclei can be obtained by averaging away the second-order quadrupolar broadening by means of double rotation (DOR),[2] dynamic angle spinning (DAS),[3] multiple-quantum magic-angle spinning (MQMAS),[4] or satellite-transition magic-angle spinning (STMAS).[5] MQMAS is the most widely used method due to its technical simplicity. The use of MAS, however, nullifies the second-rank anisotropic interactions such as the chemical shift anisotropy (CSA) and dipolar interactions. Knowledge of these would provide valuable information about the electronic environment and structural connectivity.

For a heteronuclear spin pair $I-S$ with $I = {}^1/_2$, $S \geq {}^3/_2$, high-resolution NMR spectra with dipolar information can be obtained by combining the rotational echo double resonance (REDOR) technique[6,7] with MQMAS.[8] Dipolar recoupling in a homonuclear quadrupolar spin pair is more demanding due to the fact that the applied *rf* nutation fields have to compete with the much larger quadrupolar frequency. An excitation of six-quantum coherence or spin diffusion in a pair of dipole coupled spins $S = {}^3/_2$ has been discussed in the context of MQMAS.[9,10] Three-dimensional (3D) dynamic-angle correlation spectroscopy (DACSY)[11] yields isotropic shift, characteristic for each chemical site, as well as the second- and fourth-rank anisotropic terms, which contain the principal values and relative orientations of both the CSA and quadrupolar interactions. This method is technically demanding due to the use of two rotational angles.

In this communication, we present a 3D experiment which recovers homonuclear dipolar (HMD) interaction and the CSA, while retaining site-specific resolution by combining rotary resonance recoupling (R^3)[12,13] with the MQMAS experiment. Homonuclear dipolar coupling can be selectively recoupled within the central transition without contributions from CSA, heteronuclear dipolar coupling, or quadrupolar coupling for half-integer quadrupolar nuclei at the rotary resonance (RR) condition $\omega_{rf} = \omega_r/(2S + 1)$.[14] Baldus et al. used mixing at the transverse mode in a 2D homonuclear correlation experiment that yields cross-peaks,[14] whereas in our experiment longitudinal mixing is incremented in an indirect time domain yielding an explicit dipolar Pake pattern. The advantage of longitudinal mixing over transverse mixing is that only T_1 relaxation is present during the RR mixing period. A calibration experiment is required to identify the relative sizes of spinning speed and rf intensity during the spin-locking of the central transition coherence (CTC) that determine the various RR conditions.[15] Only double-quantum coherence terms can be reintroduced into the effective Hamiltonian at $\omega_{rf} = \omega_r/4$. Figure 1A shows the 3D sequence applied to homonuclear dipolar recoupling for $S = {}^3/_2$ nuclei; the longitudinal mixing pulse is incorporated in a *z*-filtered version of the MQMAS experiment.[16] The triple-quantum coherence (TQC) excited by the first hard pulse evolves during t_1 and is converted into zero-quantum coherence (ZQC) by another hard pulse before undergoing a RR mixing at $\omega_{rf} = \omega_r/4$ for dipolar recoupling during t_2. Finally, the acquisition of the CTC during t_3 is carried out after applying a $\pi/2$ detection pulse. Hypercomplex phase cycling[17] was applied to p_1 together with CYCLOPS[18] phase cycling at p_3 to give a purely absorptive line shape. Figure 1B shows the 3D dipolar R^3 MQMAS spectrum for bis(pinacolato)diboron (BPDB) with an isolated ^{11}B-^{11}B spin pair. The 2D projection onto the F_1-F_2 plane provides the dipolar Pake pattern of each site while

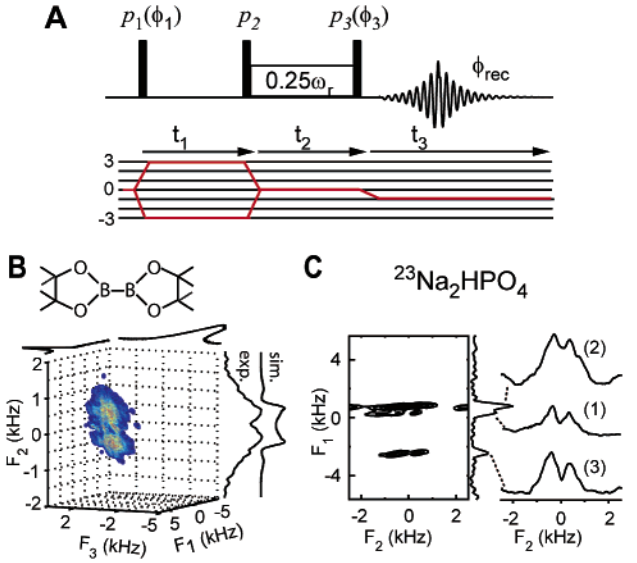

Figure 1. 3D experiment combining MQMAS with longitudinal mixing at $\omega_{rf} = \omega_r/4$. (A) The pulse sequence used in the experiment. The phase cycling was as follows: $\phi_1 = (0°, 60°, 120°, 180°, 240°, 300°)_4$; $\phi_3 = (0°)_6, (90°)_6, (180°)_6, (270°)_6$; $\phi_{rec} = (0°, 180°)_3, (90°, 270°)_3, (180°, 0°)_3, (270°,90°)_3$. A hypercomplex data set was obtained by collecting, for each t_1, a complementary set of 24 FID's with $\phi_1 = (30°, 90°, 150°, 210°, 270°, 330°)_4$. All the pulses were rotor synchronized; t_1 and t_3 were incremented with the rotor period τ_r and t_2 with $4\tau_r$. (B) Spectrum measured for BPDB with an isolated $^{11}B-^{11}B$ pair. Top view onto the F_1-F_3 plane provides a normal 2D MQMAS spectrum and side view onto the F_1-F_2 plane renders the 2D site-specific dipolar spectrum. Both experimental and simulated dipolar spectra are compared. (C) ^{23}Na 3D dipolar R^3 MQMAS measured on Na_2HPO_4. The 2D projection onto the F_1-F_2 plane shows site-specific dipolar coupling information for all three sites. All the spectra were taken at 11.7 T with a 3.2-mm rotor spinning at 20 kHz.

* To whom correspondence should be addressed. E-mail: pines@cchem.berkeley.edu.

† Presented in part at the 43rd ENC meeting (Poster no. W/T 066), Asilomar, CA, April 14−19, 2002.

10.1021/ja027043v CCC: $22.00

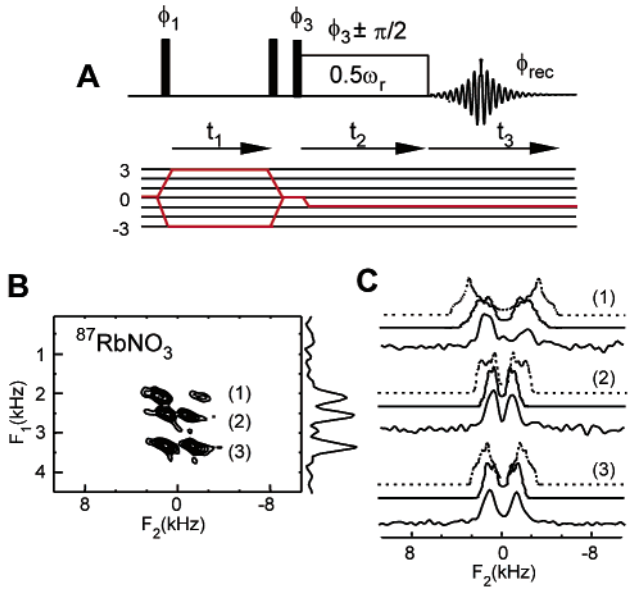

Figure 2. 3D R^3 MQMAS experiment with a RR mixing at $\omega_{rf} = \omega_r/2$. (A) A hypercomplex acquisition was performed to provide purely absorptive peaks in the MQMAS dimension. A transverse mixing pulse with $\omega_{rf} = \omega_r/2$ was applied during t_2 before direct NMR acquisition during t_3. The same phase cycling scheme was used as in Figure 1. (B) 2D projection onto the F_1-F_2 plane obtained from the 3D CSA R^3 MQMAS spectrum of $RbNO_3$. F_1 provides the isotropic spectrum, and F_2 provides CSA information. (C) Anisotropic projections for each site. Simulations with (solid line) and without (dashed line) CSA were also included. A small positive value of the CSA leads to a reduction of the line width caused by the second-order quadrupolar interaction. Inclusion of CSA explains the recoupled line width of each site (site 1: $C_Q(e^2qQ/2\pi\hbar) = 2.4$ MHz, $\eta_Q = 0.7$, $\delta_{CSA} = 46$ ppm, $\eta_{CS} = 0.4$, $\{45°, 15°, 45°\}_{CSA\to Q}$; site 2: $C_Q = 1.8$ MHz, $\eta_Q = 0.3$, $\delta_{CSA} = 28$ ppm, $\eta_{CS} = 0.6$, $\{0°, 25°, 60°\}_{CSA\to Q}$; site 3: $C_Q = 1.9$ MHz, $\eta_Q = 0.5$, $\delta_{CSA} = 31$ ppm, $\eta_{CS} = 0.5$, $\{90°, 15°, 45°\}_{CSA\to Q}$).[11]

the 2D projection onto the F_1-F_3 plane gives the usual MQMAS spectrum. The measured line width of the dipolar Pake pattern of the $^{11}B-^{11}B$ pair obtained along F_2 is ~1.3 kHz. This agrees well with a simulated line shape with a dipolar coupling constant D_{zz} of 2.5 kHz (1.71 Å),[19] scaled by the factor $3D_{zz} \sin 2\beta/4\sqrt{2}$, which is also known for double quantum recoupling in a homonuclear spin-$^1/_2$ pair,[20] where $D_{zz} = (\mu_0/4\pi)(\gamma^2h/r^3)$ and β is the angle relating dipolar vector to the rotor fixed frame. Figure 1C shows the site-specific dipolar projection of a 3D dipolar R^3 MQMAS spectrum obtained for Na_2HPO_4. The three different sodium sites of this compound are well-resolved, and the homonuclear dipolar Pake patterns are evident along the F_2 dimension. The complicated network of sodium sites, however, makes a quantitative interpretation difficult.[14]

RR conditions defined by $\omega_{rf} = n\omega_r/2$ ($n = 1, 2$) can also be included in the MQMAS pulse sequence. These conditions do not possess any selectivity for the recoupling of different types of anisotropic interactions such as CSA, dipolar coupling, and the second-order quadrupolar interaction. The dipolar influences at these modes are, however, not usually significant compared to the size of the second-order quadrupolar interaction and CSA due to the small magnetogyric ratio, possibly the low natural abundance of quadrupolar nuclei involved, or both. Moreover, the influence of the second-order quadrupolar interaction can be exactly determined on the basis of the 1D MAS or MQMAS spectra. Therefore, the CSA can be estimated from the deviation of the line shape in the recoupled spectrum from the one expected for a pure quadrupolar interaction. Figure 2A shows the 3D R^3 MQMAS pulse sequence used to obtain the additional CSA information of half-integer quadrupolar nuclei. The TQC evolving during t_1 is converted to CTC and is subjected to the RR mixing at $\omega_{rf} = n\omega_r/2$ ($n = 1, 2$) during t_2 before direct detection in t_3. A *z*-filtered MQMAS version with a hypercomplex cycling of the TQC excitation pulse was employed together with CYCLOPS phase cycling for the conversion pulse. Figure 2B shows the 2D projection onto the F_1-F_2 plane of the ^{87}Rb 3D CSA R^3 MQMAS spectrum of $RbNO_3$ at 7.05 T. All three Rb sites are resolved and exhibit the recoupled anisotropic line shapes. Figure 2C shows the projections of each Rb site along the anisotropic dimension that represent recouplings of the CSA and the second-order quadrupolar interaction obtained with $\omega_{rf} = \omega_r/2$. All dipolar interactions were ignored in the present case. Numerical simulations with (solid line) and without (dotted line) CSA for all three sites of $RbNO_3$ are also provided in Figure 2C (see figure caption for the tensor parameters). The CSA values and the relative orientations between CSA and quadrupolar tensors of $RbNO_3$ from the 3D DACSY experiment[11] show good agreement with our 3D R^3 MQMAS measurement. Inclusion of the CSA into the simulations leads to narrower line shapes than those with only the quadrupolar interaction because a positive value of the CSA leads to a cancellation effect with respect to the second-order quadrupolar term.[21]

R^3 incorporated in the MQMAS experiment enables the observation of homonuclear dipolar coupling and the CSA of half-integer quadrupolar nuclei with site-specific resolution. Such information is valuable in extracting distance- and orientation-dependent information about the structure of molecules and materials. A separate manuscript is in press which explains all of the RR conditions for anisotropic recoupling for half-integer quadrupolar nuclei.[21]

Acknowledgment. This work was supported by the Director, Office of Science, Office of Basic Energy Sciences, Materials Sciences Division, of the U.S. Department of Energy under Contract No. DE-AC03-76SF00098. H.H. thanks the Alexander von Humboldt Foundation for a postdoctoral fellowship.

References

(1) Harris, R. K.; Mann, B. E. *NMR and the Periodic Table*; Academic Press: New York, 1970.
(2) Samoson, A.; Lipmaa, E.; Pines, A. *Mol. Phys.* **1988**, *65*, 1013.
(3) Mueller, K. T.; Sun, B. Q.; Chingas, G. C.; Zwanziger, J. W.; Terao, T.; Pines, A. *J. Magn. Reson.* **1990**, *86*, 470.
(4) Frydman, L.; Harwood, J. S. *J. Am. Chem. Soc.* **1995**, *117*, 5367.
(5) Gan, Z. H. *J. Am. Chem. Soc.* **2000**, *122*, 3242.
(6) Gullion, T.; Schaefer, J. *J. Magn. Reson.* **1989**, *81*, 196.
(7) Fyfe, C. A.; Mueller, K. T.; Grodney, H.; Wong-Moon, K. C. *Chem. Phys. Lett.* **1992**, *199*, 198.
(8) Fernandez, C.; Lang, P. D.; Amoureux, J. P.; Pruski, M. *J. Am. Chem. Soc.* **1998**, *120*, 2672.
(9) Duer, M. J. *Chem. Phys. Lett.* **1997**, *277*, 167.
(10) Dowell, N. G.; Ashbrook, S. E.; McManus, J.; Wimperis, S. *J. Am. Chem. Soc.* **2001**, *123*, 8135.
(11) Medek, A.; Sachleben, J. R.; Beverwyk, P.; Frydman, L. *J. Chem. Phys.* **1996**, *104*, 5374.
(12) Oas, T. G.; Griffin, R. G.; Levitt, M. H. *J. Chem. Phys.* **1988**, *89*, 692.
(13) Vosegaard, T.; Florian, P.; Massiot, D.; Grandinetti, P. J. *J. Chem. Phys.* **2001**, *114*, 4618.
(14) Baldus, M.; Rovnyak, D.; Griffin, R. G. *J. Chem. Phys.* **2000**, *112*, 5902.
(15) Sun, W.; Stephen, J. T.; Potter, L. D.; Wu, Y. *J. Magn. Reson., Ser. A* **1995**, *116*, 181.
(16) Amoureux, J. P.; Fernandez, C.; Steuernagel S. *J. Magn. Reson., Ser. A* **1996**, *123*, 116.
(17) States, D. J.; Haberkorn, R. A.; Ruben, D. J. *J. Magn. Reson.* **1982**, *48*, 286.
(18) Hoult, D. I.; Richards, R. E. *Proc. R. Soc. (London)* **1975**, *A344*, 311.
(19) Nöth, H.; *Z. Naturforsch.* **1984**, *B39*, 1463.
(20) Nielsen, N. C.; Bildsoe, H.; Jakobsen, H. J.; Levitt, M. H. *J. Chem. Phys.* **1994**, *101*, 1805.
(21) Wi, S.; Logan, J. W.; Sakellariou, D.; Walls, J. D.; Pines, A. *J. Chem. Phys.* **2002**. In press.

JA027043V